scientific reports

Check for updates

OPEN

In vitro antiviral activities of thymol and Limonin against influenza a viruses and SARS-CoV-2

Gomaa Mostafa-Hedeab[1,17]✉, Akram Hegazy[2,17], Islam Mostafa[3], Ibrahim H. Eissa[4], Ahmed M. Metwaly[5], Hany Abdelfattah Elhady[6], Abozer Y. Eledrdery[7], Sager Holyl Alruwaili[8], Alaa Oqalaa E. Alibrahim[9], Fawaz O. Alenazy[7], Muhannad Faleh Alanazi Alruwaili[10], Thamer Alshami Marghel[11], Muharib Alruwaili[7], Alaaeldin Mohamed Saad[12,13], Mahmoud Bayoumi[13,14], Assem Mohamed El-Shazly[3,15], Luis Martinez-Sobrido[13]✉ & Ahmed Mostafa[13,16]✉

Emerging and re-emerging respiratory viruses represent a continuing threat to human health. The pandemic severe acute respiratory syndrome coronavirus-2 (SARS-CoV-2) and influenza A viruses (IAVs) are co-circulating, presenting serious threats to public health. Therefore, screening for safe and broad-spectrum antiviral candidates to control such viral infections is prioritized. Herein, this study reports the in vitro antiviral activity of some essential volatile oils (EOs) and volatile oil components including Peppermint oil, Eucalyptus oil, Clove oil, Thymol, Camphor and Limonin against two different IAVs, namely influenza A/H1N1 and A/H5N1 viruses, and SARS-CoV-2 virus. All tested samples were safe in MDCK and Vero E6 cell lines with CC_{50} values that exceed 1 mg/ml, allowing the screening of their antiviral activities using a wide range of concentrations. The results show the potency of Thymol and Limonin against influenza A/H1N1 virus with IC_{50} values of 0.022 and 4.25 µg/ml, respectively. The anti-influenza activities of Thymol and Limonin were further validated by testing them against the avian influenza A/H5N1 virus, resulting in anti-influenza activities with IC_{50} values of 18.5 and 15.6 ng/ml, respectively. The broad-spectrum potential of the highly potent antiviral candidates, Thymol and Limonin, were further tested against the pandemic SARS-CoV-2 and, both exerted anti-coronavirus activities with IC_{50} values of 0.591 and 4.04 µg/ml, respectively. Further investigations against influenza A/H1N1 virus revealed that Thymol and Limonin could inhibit IAV by hindering viral replication. The Biochemical analyses of the interaction of Limonin and Thymol with FDA-approved anti-influenza drug targets, neuraminidase and viral polymerases, revealed that both compounds can partially inhibit IAV polymerase activity, but have no effect on neuraminidase activity. Likely, molecular docking studies indicated that Thymol and Limonin obstruct active binding sites of IAV polymerases. These findings presented on the antiviral activity of Limonin and Thymol might be used to support the development of supplemental therapy against currently emerging and reemerging respiratory viral infections.

Keywords Respiratory viruses, SARS-CoV-2, IAV, Essential oils, Limonin, Thymol

[1]Pharmacology Department and Health Research Unit, Medical College, Jouf University, Skaka 11564, Saudi Arabia. [2]Department of Agricultural Microbiology, Faculty of Agriculture, Cairo University, Giza district 12613, Giza, Egypt. [3]Department of Pharmacognosy, Faculty of Pharmacy, Zagazig University, Zagazig 44519, Egypt. [4]Medicinal Chemistry Department, Faculty of Pharmacy (Boys), Al-Azhar University, Cairo 11884, Egypt. [5]Pharmacognosy and Medicinal Plants Department, Faculty of Pharmacy (Boys), Al- Azhar University, Cairo 11884, Egypt. [6]Surgery Department, Medical College, Jouf University, Sakaka 11564, Saudi Arabia. [7]Department of Clinical Laboratory Sciences, College of Applied Medical Sciences, Jouf University, Sakaka 11564, Saudi Arabia. [8]Department of Surgery, Orthopedic Division, College of Medicine, Jouf University, Sakaka 11564, Saudi Arabia. [9]Department of Internal Medicine, College of Medicine, Jouf University, Sakaka, Saudi Arabia. [10]Department of Internal Medicine, Division of Radiology, College of Medicine, Jouf University, Kingdom of Saudi Arabia, 72388 Sakaka, Saudi Arabia. [11]Department of Pediatrics, College of Medicine, Jouf University, Jouf University, Kingdom of Saudi Arabia, 72388 Sakaka, Saudi Arabia. [12]Department of Zoonoses, Faculty of Veterinary Medicine, Zagazig University, Zagazig, Egypt. [13]Disease Intervention & Prevention (DIP) and Host Pathogen Interactions (HPI), Texas Biomedical Research Institute, Programs, San Antonio, TX 78227, USA. [14]Virology Department, Faculty of Veterinary Medicine, Cairo

University, Giza, Egypt. [15]Faculty of Pharmacy, El Saleheya El Gadida University, El Saleheya El Gadida, Sharkia 44813, Egypt. [16]Center of Scientific Excellence for Influenza Viruses, National Research Centre, Giza 12622, Egypt. [17]Gomaa Mostafa-Hedeab and Akram Hegazy contributed equally to this work. ✉email: gomaa@ju.edu.sa; lmartinez@txbiomed.org; ahmed_elsayed@daad-alumni.de

The current COVID-19 pandemic is a compelling verification that respiratory viruses including influenza A viruses (IAVs) and coronaviruses (CoVs) pose serious threats to public health. Different sectors of vital roles in society such as the economy, education, and healthcare have been negatively impacted since early 2020 due to this devastating COVID-19 pandemic[1]. Other respiratory viruses including seasonal and avian IAVs have a substantial global influence on morbidity and mortality, particularly in young children[2,3]. Acute respiratory distress syndrome (ARDS) accounts for approximately 20% of all childhood deaths globally, especially among underprivileged communities in tropical areas where the case fatality rates due to ARDs can be noticeably greater than in temperate areas of the world[4]. Mild respiratory illnesses, acute viral pneumonia, and even complete respiratory collapse are all diseases that are linked to infections caused by respiratory viruses[5].

Human respiratory viruses including respiratory syncytial virus (RSV), human coronavirus (HCoV), human bocavirus (HBoV), parainfluenza virus, rhinovirus, adenovirus, and metapneumovirus are the gangsters of respiratory infections and they are known to be well-adapted with person-to-person transmission potentiality and can circulate frequently across all age groups[6]. In addition, IAVs such as influenza A/H1N1, A/H3N2, and A/H5N1, and HCoV including SARS-CoV, MERS-CoV and SARS-CoV-2 have become the most health-threatening viruses causing a high global concern[7]. The etiological agent of the world's first pandemic event was the influenza A/H1N1 virus, where a frightening and catastrophic pandemic struck the entire globe in three successive waves between 1918 and 1919 resulting in about 50 million deaths all over the world[8]. IAVs are contagious as the viruses' transmissibility from person to person is extremely high. Additionally, IAV's case-fatality rates (CFR; the percentage of people who are diagnosed with a particular disease and die from it) during pandemic events are quite high[9–11]. Since late December 2019, the world has been battling the brand-new CoVs known as SARS-CoV-2 which is presently producing a historic pandemic of coronavirus disease-19 (COVID-19)[12].

Vaccination is considered the bedrock of preventative measures for respiratory viral infections, however, due to the propensity of some viruses to evolve and evade the immune system (e.g., IAV and SARS-CoV-2), vaccines must be redesigned[13–15]. Additionally, a typical vaccine supply chain is unavailable, and vaccination alone cannot stop fast-spreading pandemics and outbreaks[16]. This necessitates the preparedness for upcoming pandemic events through different prophylactic approaches such as antiviral therapies. To alleviate this issue, drug repurposing studies have been conducted on many FDA-approved medications to test their efficacy against IAVs and SARS-CoV-2[17–20]. Concurrently, plant-based medicines are being investigated to counteract these respiratory infections. Nature has long been recognized as the primary source of drug development where almost 65% of the total 1,211 novel small-molecule medications approved between 1981 and 2014 were developed directly or indirectly from natural sources[21]. In this context, plant-based extracts and bioactive phytochemicals showed high safety and great potential to effectively control viral infections[22–24].

Essential oils (EOs) are a group of phytochemicals that are being intensively investigated since they possess a diverse range of pharmacological activities, such as antimicrobial, antibacterial, antiviral, antiparasitic, and insecticidal capabilities[25,26]. They consist of a variety of chemical substances including aldehydes, terpenes, terpenoids, and phenylpropanoids[27–29]. Since they are safe and non-toxic, they belong to a group of phytochemicals called GRAS (generally recognized as safe) which represents an advantage over chemically synthesized drugs[30]. The efficacy of EOs in the treatment of acute, contagious, and chronic diseases has been previously reported[31–34]. Herein, the antiviral activities and relative cytotoxic potentials of commercially available purified EOs or components against diverse respiratory viruses, including influenza A/H1N1 and A/H5N1, and SARS-CoV-2 were investigated to pave the way to discover novel and safe broad-spectrum supplementary interventions to control IAV and SARS-CoV-2 infections.

Materials and methods

Cell lines and viruses

The Madin Darby Canine Kidney (MDCK) (ATCC, CCL-34), human embryonic kidney (293T) (ATCC, CRL-3216) and clone 6 of the African green monkey kidney (Vero E6) (ATCC, CRL-1586) cells were cultured in growth Dulbecco's modified Eagle's medium (DMEM; BioWhittaker, Walkersville, MD, USA), supplemented with 1% Penicillin/Streptomycin (pen/strep) mixture (GIBCO-BRL; New York, USA) and 10% fetal bovine serum (FBS) (Gibco-BRL; New York, USA).

The highly pathogenic avian influenza A/chicken/Egypt/N12640A/2016 (H5N1) virus and the seasonal human influenza A/Egypt/NRC098/2019 (H1N1) virus (GISAID ID: EPI ISL 12995118) were propagated in embryonated chicken eggs specific pathogen-free (ECE-SPF) and MDCK cells, respectively. The SARS-CoV-2 strain, hCoV-19/Egypt/NRC-3/2020[35], was propagated in Vero E6 cells. Cell culture supernatants were further harvested, and clarified from cell debris by centrifugation and the supernatant was aliquoted and then kept at -80 °C as stocks until further use. To evaluate viral load in stored virus aliquots, Reed and Muench's median tissue culture infectious dose ($TCID_{50}$) assay was performed to estimate specific viral dilutions that can induce 50% CPE in the cell lines[36].

Essential volatile oils (EOs) and EOs-derived components

Eucalyptus oil was purchased from FREY&LAU GmbH (Henstedt-Ulzburg, Germany). Peppermint and clove oils were obtained from Kamena (Giza, Egypt, purity = 99.5%). Thymol was purchased from MERCK (Darmstadt, Germany, purity ˃ 99%) and Camphor was purchased from research lab fine chem industries (Mumbai, India, purity ˃ 99%). Eventually, Limonin was extracted by Hamdan and her colleagues as previously described (purity > 97%)[37] (Table 1).

Cytotoxicity and viral Inhibition activity

Crystal violet assay was employed to evaluate the cytotoxicity of the investigated EOs on MDCK or Vero E6 cells through the determination of the half-maximal cytotoxic concentration (CC_{50}) and also to depict the anti-influenza and anti-coronavirus activities of these phytochemicals against IAVs and SARS-CoV-2 by calculating the half maximal inhibitory concentration (IC_{50})[59,60].

To determine the CC_{50}, 3×10^5 cells/mL of MDCK or Vero E6 were first seeded in 96-well plates and incubated in a humidified CO_2 incubator at 37 °C overnight to form 80–90 confluent cell monolayers. The confluent cell monolayers were washed with 1X phosphate-buffered saline (PBS), and then tenfold serial dilutions of these EOs (in triplicates) were added to the plates. Untreated cell monolayers were included as cell control. The plates were then incubated for 3 days at 37 °C under 95% humidity and 5% CO_2 conditions. After the incubation period, the fixation step was applied using the fixing solution (10% paraformaldehyde, PFA). About 1 h later, visualization using 0.1% crystal violet stain was performed. The stained cells were then washed thoroughly, and dried overnight, and then 200 µl of absolute methanol were added to each well and the plates were shaken for 25 min on a bench rocker to dissolve the crystal violet stain for further optical density (OD) measurement. The microplate reader was used to detect the OD at a wavelength of 570 nm. GraphPad Prism software (version 5.01) was used to perform nonlinear regression analysis to determine the CC_{50} values by graphing log concentrations of each EOs against the normalized response (variable slope).

To determine the IC_{50}, 3×10^5 cells/mL of MDCK or Vero E6 were first seeded in 96-well plates and incubated in an incubator at 37 °C under 95% humidity and 5% CO_2 conditions. The next day, the cells were washed with 1X PBS, and virus adsorption was allowed by a mixture of 100 µl DMEM containing each safe concentration (non-cytotoxic) and 100 $TCID_{50}$ of each virus per well. The virus and cell control wells were also included. The plates were then incubated at 37 °C in an incubator with 95% humidity and 5% CO_2 condition. Three days later, the 10% PFA solution was then added to inactivate the virus and fix the cell monolayers. The cell monolayers are then stained using 0.1% crystal violet staining solution for 30 min at room temperature (RT). The crystal violet stains of the fixed cells were then dissolved as previously described and the OD values were measured. The GraphPad Prism software was used to perform a nonlinear regression analysis to determine the IC_{50} values for each EO.

Plaque infectivity assay (PIA)

Plaque infectivity assay was performed to calculate countable viral titers (plaque forming unit (PFU)/ml) as demonstrated earlier, with slight changes[61,62]. Briefly, MDCK or Vero E6 cells were cultured in 6 well plates and incubated for 24 h at 37 °C with 95% humidity in a 5% CO_2 incubator. After removal of exhausted growth media and washing with 1X PBS, the 80–90% confluent cell monolayers were then infected with serial tenfold dilutions of each virus for 1 h. Afterwards, the infection media comprises 1X DMEM enriched with 4% bovine serum albumin (BSA; Gibco-BRL; New York, USA), 1% antibiotic/antimycotic mixture (penicillin/streptomycin) and 1 µg/mL of L-1-tosyl- amido-2-phenylethyl chloromethyl ketone (TPCK)-treated trypsin. The plates were then incubated for 1 h to allow viruses to adsorb onto their corresponding host cell receptors. During the incubation, the plates were shaken gently to make the viral particles equally distributed over the cell monolayer. Following incubation, the un-adsorbed particles were discarded, and the cells were then overlayed with 3 ml of overlay medium (1% agarose, 1X DMEM enriched with 0.3% BSA, 1% penicillin/streptomycin, and 1 µg/mL TPCK-treated

Essential Oil (EO)	Plant Family	Reported Biological Activities	Reported Sensitive Viruses	Specific Gravity (25 °C)	Citation(s)
Peppermint oil	Lamiaceae	Antiviral and broad-spectrum antibiotic	HSV-1 and HSV-2	0.916 g/mL	38–40
Eucalyptus oil	Myrtaceae	Antiviral and antimicrobial	IAV (A/H1N1 ATCC VR-R 1520) and MV	0.923 g/mL	41,42
Clove oil	Myrtaceae	antitumor, antimicrobial, anti-inflammatory, and antiviral	HSV-1 and HSV-2	1.06 g/mL	38–40,43–45
Thymol	Lamiaceae, Apiaceae, and Orobanchaceae	Antiseptic, antimicrobial, anticarcinogenic and antiviral	HSV-1 and SARS CoV-2 and IAV (H1N1; A1/Denver/1/57)	0.965 g/mL	46–49
Camphor	Lauraceae	Antipruritic, antiseptic, antibacterial and antiviral (Camphor derivatives)	IAV and VV	0.99 g/mL	50,51
Limonin	Rutaceae	Antiviral, anti-inflammatory, antibacterial, anti-cancer, antioxidant, analgesic, nerve protection, liver protection, and blood lipid regulation	NDV, HSV-1, HSV-2 HIV-1, and SARS CoV-2	1.39 g/mL	52–58

Table 1. Investigated essential oils, plant origin, and their reported biological activities. IAV: influenza A virus; SARS CoV-2: severe acute respiratory syndrome coronavirus-2; VV: vaccinia virus; HSV-1: herpes simplex virus type 1; HSV-2: herpes simplex virus type 2; MV: mumps virus; NDV: Newcastle disease virus.

trypsin). The plates were then allowed to set before incubating them for three days at 37 °C under 95% humidity and 5% CO_2 conditions. The same fixation and visualization procedures using 0.1% crystal violet staining solution were finally applied to visualize the plaques for counting them. The following equation was used to calculate the viral titer for each virus as expressed in PFU/ml:

$$Virus\ titer\ (\mathrm{PFU/mL}) = \text{Number of plaques X Reciprocal of virus dilution X Dilution factor (to reach 1 ml)}$$

Plaque reduction assay (PRA)

To further confirm the antiviral activities of effective phytochemicals, the plaque reduction assay was performed in MDCK or Vero E6 cell monolayers in a six-well plate as previously described[60] with minor modifications. Briefly, the 1.2×10^6 cells were cultured per well for 24 h at 37 °C under 95% humidity and 5% CO_2 conditions. The virus was diluted to a countable number of viral plaques per well (predefined using PIA) and mixed with the nontoxic concentration of EOs and incubated for 1 h at 37 °C before being added to the confluent cell monolayers. Growth medium was aspirated, and the cell monolayers were inoculated with 100 µL/well of the co-incubated virus with the EOs and incubated for 1 h to allow infectious viral particle adsorption. The cell monolayers were then washed with 1X PBS and supplemented with 3 ml of the overlay medium. The plates with solidified overlays were then incubated at 37 °C until the formation of viral plaques for 3 days. The cell fixing solution (4% paraformaldehyde (PFA)) was added to the overlay for 1 h to inactivate the remaining viral particles and fix the cell monolayers. The plates were then stained with 0.1% crystal violet. The plaques were then counted, and the percentage of viral reduction was then calculated in relative to virus control wells as following:

$$\text{Virus reduction}\ (\%) = \frac{(\text{Untreated virus count} - \text{Treated virus count})}{\text{Untreated virus count}}\ \text{X}\ 100$$

Stages of the antiviral action

To investigate the potential stages at which Thymol and Limonin could impair the viral replication cycle, we assessed three possible stages, including (i) inhibiting the viral replication, (ii) interfering with viral particle adsorption onto the host cell receptor or (iii) targeting the virus away from the host cell (cell-free effect or virucidal effect), modified plaque reduction protocol has been used as previously described[60] to recognize the potential viral/cell-based target.

Interference with viral replication cycle stages

MDCK or Vero E6 were cultured into 6-well culture plates and incubated at a humidified 5% CO2 incubator. The next day, 100 µl of the infectious viral dilutions for each virus were added to each well with 80–90% confluent cell monolayers. The cell and virus controls ($n = 3$) were included, and the plates were then incubated for 1 h at 37 °C under 95% humidity and 5% CO_2 conditions to allow viral adsorption. Following viral infection, the un-adsorbed viral particles were washed away using the 1X PBS solution. Immediately, 100 µl of different non-cytotoxic concentrations from Thymol and Limonin were added to each well except controls and the plates were incubated at the same conditions for another 1 h. Another washing step with 1X PBS solution was applied and the cells were covered with 3 ml of the predefined overlay media. After three days of incubation at 37 °C, the cells were fixed with 100 µl of the 10% paraformaldehyde fixing solution per well for 1 h. The plates were then stained with 0.1% crystal violet stain for 10 min. Following washing the plates thoroughly with water and drying overnight, the viral plaques were counted, and viral inhibition percentages were calculated as indicated in the PRP.

Interference with viral adsorption onto cell receptors

The MDCK and Vero E6 cells were seeded in 6-well culture plates and incubated for one day at 37 °C under 95% humidity and 5% CO_2 conditions. The following day, the predetermined non-cytotoxic concentrations for Thymol and Limonin were incubated with 80–90% confluent cell monolayers for 1 h at 4 °C (to prevent sample internalization through cell membrane pores). The cell and virus control wells were included. After the incubation, 1X PBS solution was used to wash away the un-adsorbed chemicals. The predefined infectious viral dilutions were then added to the chemically treated cells, and the plates were incubated for another 1 h at 37 °C under 95% humidity and 5% CO_2 conditions to allow for viral infection. Excess un-adsorbed viruses were washed away using 1X PBS and immediate addition of the overlay media was carried out. After incubating the plates for 3 days at 37 °C under 95% humidity and 5% CO_2 conditions, the same fixation, visualization, and calculations of the viral inhibition percentages were employed as in PRP.

Direct virucidal action

Predefined safe concentrations of each promising essential oil were mixed up with concentrated viruses (3–4 times higher than the viral dilution with countable viral plaques) and incubated at 37 °C for 1 h. Following that, a 3–4 times serial decimal dilution was used to achieve a countable titer of influenza A/H1N1. The virus/compound mixture (containing countable viral titer and negligible concentrations of each essential oil) was added to monolayers of MDCK cells that were 80–90% confluent in 6-well plates. This treatment lasted for 1 h at 37 °C under 95% humidity and 5% CO_2 conditions. After the incubation, the cells were washed with 1X PBS solution, covered with 3 ml of overlay medium, and incubated for 72 h

at 37 °C. Likewise, the viral inhibition percentages were calculated after the same fixation, visualization, and calculation methods used in the plaque reduction protocol.

Biochemical analyses

Minigenome assay of the polymerase activity

For polymerase activity assay, the sets pHW000 plasmid DNA expressing the PB2, PB1, PA and NP proteins that constitute the influenza A/H1N1 viral ribonucleoprotein complex (vRNP) components were used together with pPOLI-ZsG-NLuc plasmid expressing the vRNA-like transcript of ZsGreen and nanoluciferase reporters[63]. In HEK 293T cells, 1 µg of each plasmid (total 5 µg of plasmid DNA). The plasmids were transfected using lipofectamine 300 according to manufacturer instructions. Approximately 8 h post transfection, 2 ml of infection media containing 10 µg/ml of the Limonin or 0.1 µg/ml of the Thymol and incubated in a humidified CO_2 incubator. A Cypridina luciferase (Cluc)-expressing plasmid (1 µg) under the control of the chicken β-actin promoter in a pCAGGS plasmid was included to normalize transfection efficiencies[63]. After 24 h, the transfected cells were assed for the ZsGreen expression using EVOS M5000 Microscope and the cell culture supernatants were collected to measure the nanoluciferase activity. For the negative control set, pHW2000 blank vector was used instead of the PB2 subunit. Bioluminescence data were developed as per the manufacturer's protocol using Nano-Glo luciferase substrate (Promega, US) and Cluc substrate (ThermoFisher Scientific, US) and acquired/analyzed using the Aura program (AMI Spectrum).

Neuramindase Inhibition assay

To evaluate the impact of Limonin and Thymol on the neuraminidase activity of influenza A/H1N1, the NA-Fluor™ Influenza Neuraminidase Assay Kit (ThermoFisher Scientific) was utilized, following the manufacturer's protocol. Viral stock of influenza A/H1N1 was titrated to determine the appropriate dilution for the inhibition assay. Limonin and Thymol were tested in a series of 10-fold dilutions to evaluate their neuraminidase inhibitory activity. Zanamivir was used as a positive control and was tested across a range of concentrations (10mM-10pM). Fluorescence measurements were performed using BioTek Synergy microplate reader at an excitation of 355 nm and an emission of 460 nm. Using GraphPad Prism Software, the IC_{50} values were determined from the nonlinear regression analysis by plotting log inhibitor versus normalized response.

In Silico Docking studies

Protein Preparation

The crystal structures of influenza A/H1N1 IAV polymerase basic 2 (PB2) protein (PDB ID: 7AS0, resolution: 1.55 Å), and IAV polymerase acidic (PA) protein (PDB ID: 6FS6, resolution: 2.29 Å) were retrieved from the Protein Data Bank (https://www.rcsb.org) on 1 February 2024. Initially, the selected protein structures underwent preparation by removing crystallographic water molecules, with retention of only one chain for each protein alongside the co-crystallized ligands. Protonation of protein chains was conducted using default parameters, followed by energy minimization. Subsequently, the active pockets of various proteins were identified, considering residues within 5 Å of the co-crystallized ligand's edge as active sites[64].

Ligand Preparation

The chemical structures of the compounds under investigation were depicted using ChemBioDraw Ultra 14.0 and saved in MDL-SD file format. Subsequently, protonation and optimization were carried out through energy minimization using the MM2 force-field[65].

Docking setup and validation of Docking protocol

Docking studies were conducted using MOE version 2019. To validate the docking procedure, redocking of the co-crystallized ligands was performed against various active sites. The resulting RMSD values were calculated, with a value less than 2 Å indicating the validity of the docking processes[66].

Docking procedures were executed against the active sites, generating setups for 30 docked poses for each ligand utilizing ASE as a scoring function[67]. The pose with a favorable binding mode was then selected. Subsequent visualization was performed using Discovery Studio (DS) 4.0[68]. The comparison of the binding mode of the tested compounds with that of the reference molecules provided valuable insights into the binding patterns of the tested compounds[69,70].

Results

Cytotoxicity and viral inhibitory effects of the investigated EOs

To depict the broad-spectrum antiviral potential of specific EOs, selected based on their reported biological activities (Table 1), the antiviral activities were assessed against two IAVs (influenza A/H1N1 and A/H5N1) and SARS-CoV-2 in MDCK and Vero E6 cell lines at non-toxic concentrations. Remarkably, the cytotoxicity investigations showed that the tested EOs were safe to MDCK (Fig. 1a) and Vero E6 cells (Fig. 1b) with concentrations up to 10 mg/ml for most of them. Based on cytotoxicity findings, the

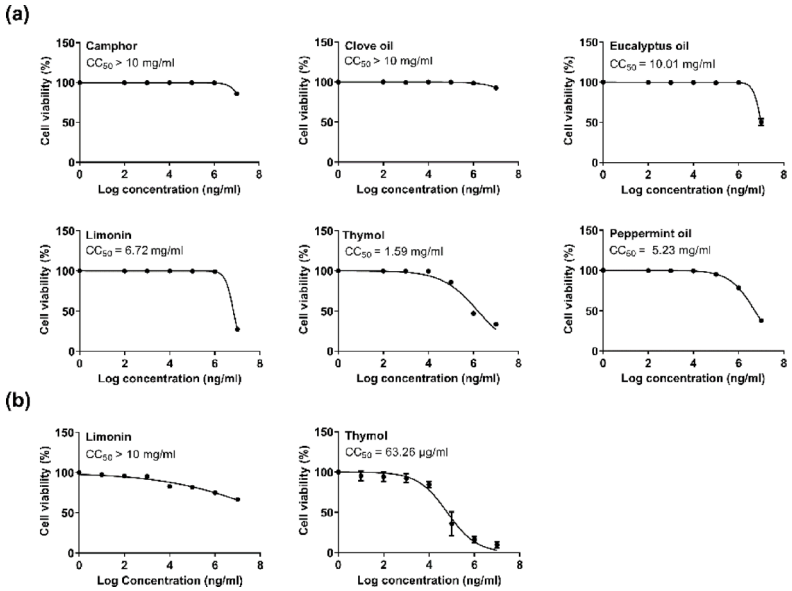

Fig. 1. Cytotoxicity of the investigated essential oils (EOs) and EOs components. (**a**) Cytotoxicity of the investigated EOs on the MDCK cell line; (**b**) Cytotoxicity of Thymol and Limonin in Vero E6 cells. By plotting log inhibitor versus normalized response (variable slope) and running non-linear regression analyses using GraphPad Prism 5.01 software, the CC_{50} values were determined.

antiviral activities of these EOs were first assessed against seasonal human influenza A/H1N1 virus and compared to FDA-approved anti-influenza reference drugs, namely Zanamivir (Fig. 2a; Table 2).

Out of the six investigated EOs, only Limonin and Thymol showed promising anti-influenza activities against the tested virus with IC_{50} values of 4.25 µg/ml and 0.022 µg/ml, respectively (Fig. 2a). On the contrary, Camphor exerted mild-to-moderate antiviral potential with an IC_{50} value of 234.1 µg/ml, while Peppermint, Eucalyptus, and Clove oils produced no antiviral effect against influenza A/H1N1 virus (Fig. 2). To confirm that the antiviral activity of EOs with high selectivity index (SI) values (Table 2) is not a strain-specific effect, Thymol and Limonin were further investigated against the avian influenza A/H5N1 virus. Likewise, Limonin and Thymol exerted potent antiviral activities against influenza A/H5N1 virus at IC_{50} values of 18.5 ng/ml and 15.6 ng/ml, respectively (Fig. 2b).

Selectivity index (SI) = half maximal cytotoxic concentration (CC_{50}) /half maximal inhibitory concentration (IC_{50}).

To investigate the antiviral activity of Limonin and Thymol against non-influenza respiratory viral pathogen, the cytotoxicity of Thymol and Limonin in Vero E6 cells and their antiviral activities against SARS-CoV-2 were evaluated. Interestingly, Limonin showed lower cytotoxicity in Vero E6 cells (CC_{50} > 10 mg/ml), while Thymol showed apparent cytotoxicity on Vero E6 (CC_{50} = 63.26 µg/ml). On the same hand, Thymol and Limonin showed effective antiviral activities against SARS-CoV-2 at IC_{50} values of 0.591 µg/ml and 4.04 µg/ml, respectively (Fig. 2c) as compared to the reference drug Remdesivir (Table 2). This confirms the broad-spectrum antiviral activity of Thymol and Limonin against different respiratory viral pathogens.

Concentration-dependent plaque reduction

The plaque reduction assay was used to validate the anti-influenza efficacy of Thymol and Limonin against human and avian influenza A viruses. The plaque reduction percentages for Thymol and Limonin typically proved the antiviral potency against both tested influenza viruses (A/H1N1 and A/H5N1) where the viral titers were reduced using low and safe concentrations of Thymol and Limonin (Fig. 3).

Potential targets for antiviral actions

It is noteworthy that there are different stages at which the candidate antiviral drugs can hit the viral replication cycle stages to combat viral infections. In this perspective, three key stages at which Thymol and Limonin could interfere with the viral replication cycle stage(s) of influenza A/H1N1 virus were investigated, including viral adsorption, viral replication cycle stages, and cell-free status of the intact virus "virucidal effect". Interestingly, both Thymol and Limonin could mainly exert their anti-influenza efficacy via interference with viral replication cycle stages (Table 3). Limonin could also affect viral adsorption, while treatment with Thymol is partially associated with a virucidal effect.

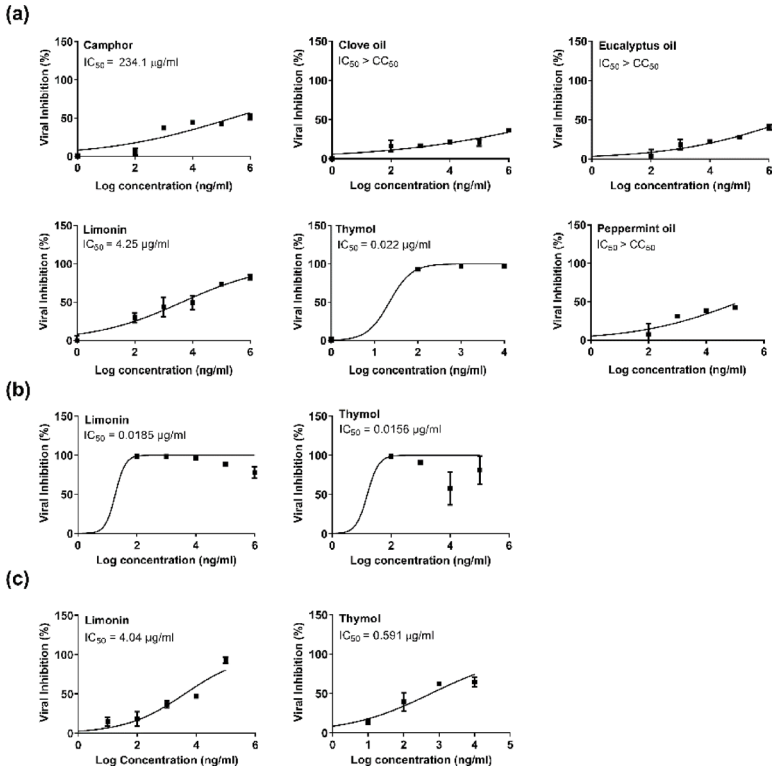

Fig. 2. Antiviral activities of the investigated essential oils (EOs) and EOs components. (**a**) Antiviral effects of the investigated EOs and EOs components against seasonal human influenza A/H1N1 virus; (**b**) Antiviral effects of Thymol and Limonin against highly pathogenic avian influenza A/H5N1 virus. (**c**) Anti-coronavirus activity against SARS-CoV-2. By plotting log inhibitor versus normalized response (variable slope) and running non-linear regression analyses using GraphPad Prism 5.01 software, the IC_{50} of the investigated EOs were determined.

Essential Oil	Virus	CC_{50} (mg/ml)	IC_{50} (µg/ml)	SI	Citations
Thymol	H1N1	1.59	0.022	> 100	This study
	H5N1		0.0156	> 100	
	SARS-CoV-2	0.0632	0.59	< 100	
Limonin	H1N1	6.72	4.25	> 100	
	H5N1		0.0185	> 100	
	SARS-CoV-2	< 10	4.04	< 100	
Camphor	H1N1	< 10	234.1	42.7	
Peppermint oil	H1N1	5.23	$IC_{50} < CC_{50}$	N/A	
Eucalyptus oil	H1N1	10.01	$IC_{50} < CC_{50}$	N/A	
Clove oil	H1N1	< 10	$IC_{50} < CC_{50}$	N/A	
Zanamivir	H1N1	< 10	0.792	> 100	[71]
	H5N1		0.265	> 100	
Remdesivir	SARS-CoV-2	0.473	6.721	70.40	[72]

Table 2. The selectivity index (SI) values of the tested essential oils against influenza A/H1N1 and A/H5N1, and SARS-CoV-2 viruses.

Biochemical experiments

To further validate the interaction between Limonin or Thymol and the viral polymerase, we conducted a minigenome assay in 293T cells using influenza A/H1N1 viral ribonucleoprotein complex proteins expressed from plasmid constructs, along with a reporter system expressing ZsGreen (ZG) and nanoluciferase (Nluc) under the control of the pol-1 promoter. Interestingly, both Limonin and Thymol showed an ability to reduce fluorescence (Fig. 4a) and nanoluciferase (Fig. 4b) expressions, however the reduction was significant with Thymol. On the same hand, the anti-neuraminidase activities of Limonin

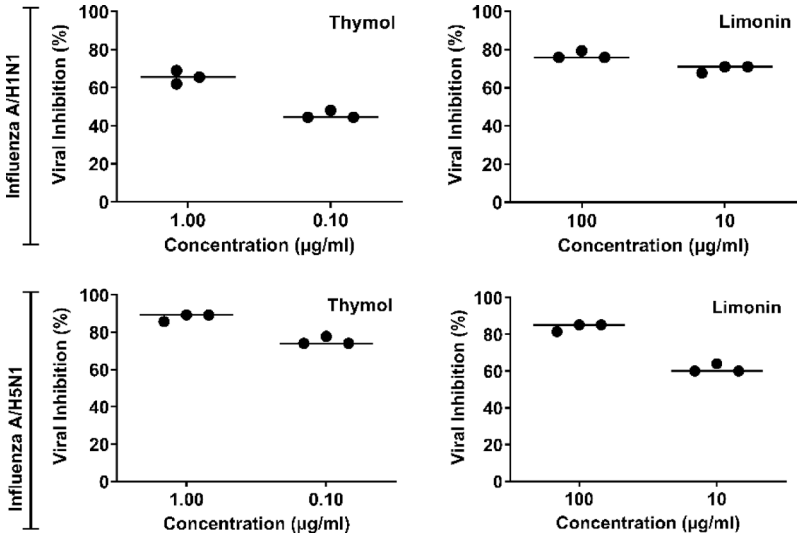

Fig. 3. Viral inhibition after treatment with two different concentrations of the highly promising essential oils as measured by plaque reduction assay. The viral reduction in influenza A/H1N1 and A/H5N1 following treatment with the two essential oils were depicted in percentages. Each oil was evaluated independently against both viruses and data were plotted using GraphPad Prism 5.01 software.

Essential Oil	Conc. (µg/ml)	Potential Targets		
		Viral replication cycle	Virucidal	Viral adsorption
Limonin	100	98.8%	43.3%	64%
	10	94%	30.9%	55%
Thymol	1	90.1%	70.4%	39.4%
	0.1	89.3%	66.7%	37.9%

Table 3. Viral Inhibition percentages following the investigation of the three potential antiviral targets as determined by conducting a modified plaque reduction protocol against influenza A/H1N1 virus in MDCK cells.

and Thymol in comparison to Zanamivir as an FDA approved neuraminidase inhibitor were tested using the neuraminidase inhibition assay and a wide range of concentrations (10mM-10pM). As expected, Zanamivir exhibited strong anti-neuraminidase activity with an IC_{50} of 21.28 pM, while limonin and thymol show very weak ability to inhibit the neuraminidase activity with an estimated IC_{50} values higher than 10mM (Fig. 4c). These findings confirm that Limonin and Thymol may partially exert their antiviral activity via direct interaction with viral polymerase, and that their anti-influenza effects are likely unrelated to neuraminidase inhibition.

Docking studies

To comprehend the antiviral activities at a molecular level, the most active compounds, Thymol and Limonin, were subjected to docking against influenza A/H1N1 IAV polymerase basic 2 (PB2) protein (PDB ID: 7AS0), and IAV polymerase acidic (PA) protein (PDB ID: 6FS6). Pimodivir and Baloxavir acid served as reference molecules against the respective proteins under examination. The efficiency of binding against the active sites was evaluated in the docking studies based on both binding mode and binding energy (Table 4).

Validation

To validate the docking process, docking procedures were executed for the co-crystallized ligands within the active sites of the tested proteins. MMFF94X served as the force field, and ASE functioned as a scoring function for protocol validation. The small RMSD values observed between the docked poses and the co-crystallized ligands during the validation step indicated the feasibility of the employed methodology for the intended docking experiments (0.32, and 0.26 Å for PB2 and PA proteins, respectively) (Fig. 5a and b).

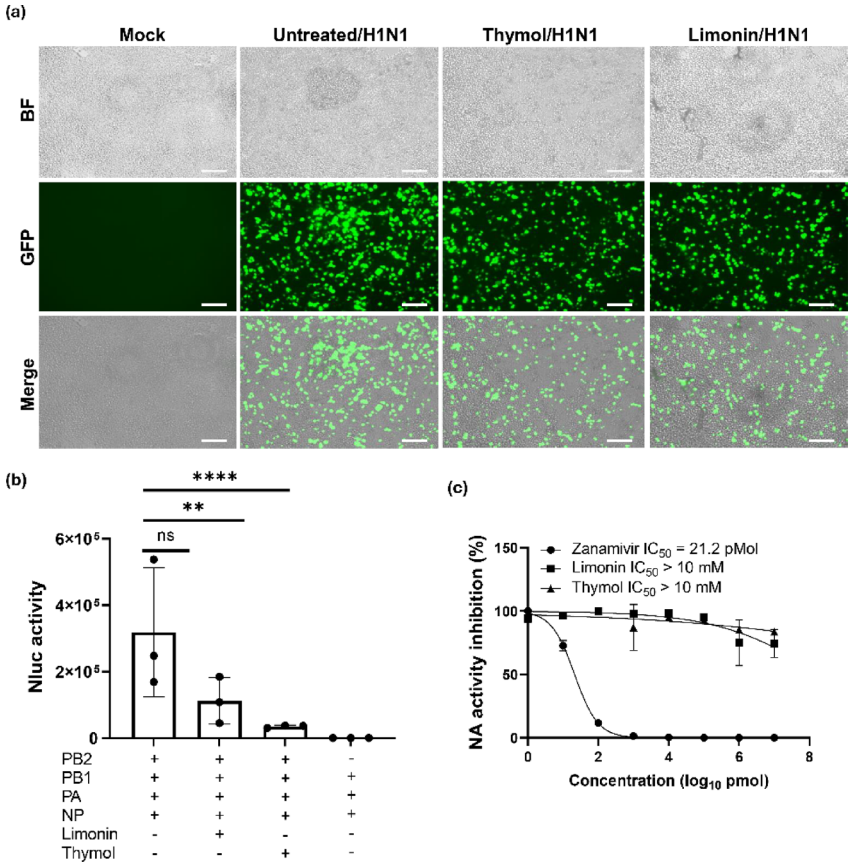

Fig. 4. Biochemical assays to explore the anti-polymerase and anti-neuraminidase activities of Limonin and Thymol. (**a**) Minigenome assay to validate possible biological interaction of Thymol and Limonin with influenza A/H1N1 polymerase subunits as determined by ZsGreen expression in treated and untreated transfected HEK 293T cells or (**b**) by measuring the nanoluciferase activity in the supernatants of treated and untreated transfected HEK 293T cells. (**c**) The neuraminidase inhibition assay against influenza A/H1N1 showed that Limonin and Thymol have a rare effect on viral neuraminidase activity.

Compound	PB2	PA
Thymol	− 18.21	− 12.52
Limonin	− 22.62	− 22.54
Pimodivir	− 22.55	–
Baloxavir acid	–	− 19.43

Table 4. Binding free energies (ΔG in Kcal/mol) of thymol and Limonin against PB2, and PA proteins as compared to the reference molecules.

Docking studies against IAV PB2 protein

The co-crystallized ligand (Pimodivir) demonstrated a binding score of -22.55 kcal/mol against IAV PB2 (RdRP subunit). The bicyclo[2.2.2]octane-2-carboxylic acid moiety occupied the first pocket of the active site, forming one hydrogen bond with Asn429. Furthermore, it engaged in four hydrophobic interactions with His432, Met431, and Phe325. Additionally, three electrostatic attractions were observed between the carboxylic group and amino acids Arg355 and His357. The fluoropyrimidine moiety was positioned in the second pocket, forming one hydrophobic bond with Phe323. Moreover, the 5-fluoro-1*H*-pyrolo[2,3-*b*]pyridine moiety occupied the third pocket, establishing four hydrogen bonds with Glu276, Arg152, Asn3Gln406, Phe404, Lys376, and Glu361. Additionally, two electrostatic attractions were formed with His357 (Fig. 6a). Thymol exhibited a binding energy of -18.21 Kcal/mol against IAV PB2 protein, forming nine hydrophobic interactions with Phe325, Met431, His357, Lys376, and Phe404 (Fig. 6b). Limonin displayed a more efficient binding mode than Thymol, with a binding energy of -22.62 Kcal/mol against IAV PB2 protein. It was positioned in three different pockets of the active site, forming one hydrogen

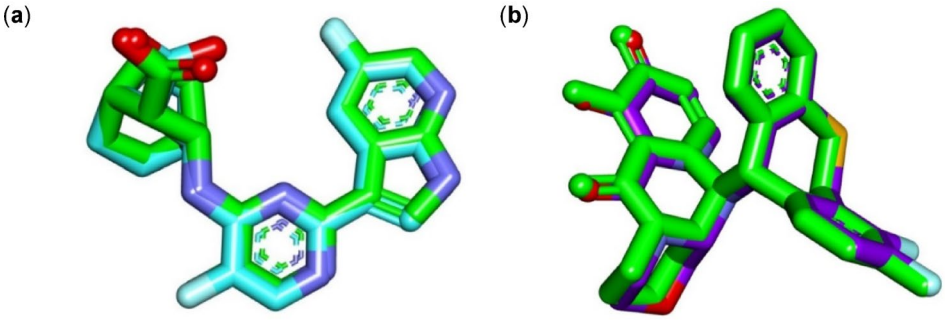

Fig. 5. (**a**) Superimposition of the co-crystallized ligand (Pimodivir) of IAV PB2 (carbon atoms in green) and the docked pose of the same ligand (carbon atoms in turquoise); (**b**) Superimposition of the co-crystallized ligand (Baloxavir acid) of IAV PA (carbon atoms in green) and the docked pose of the same ligand (carbon atoms in violet).

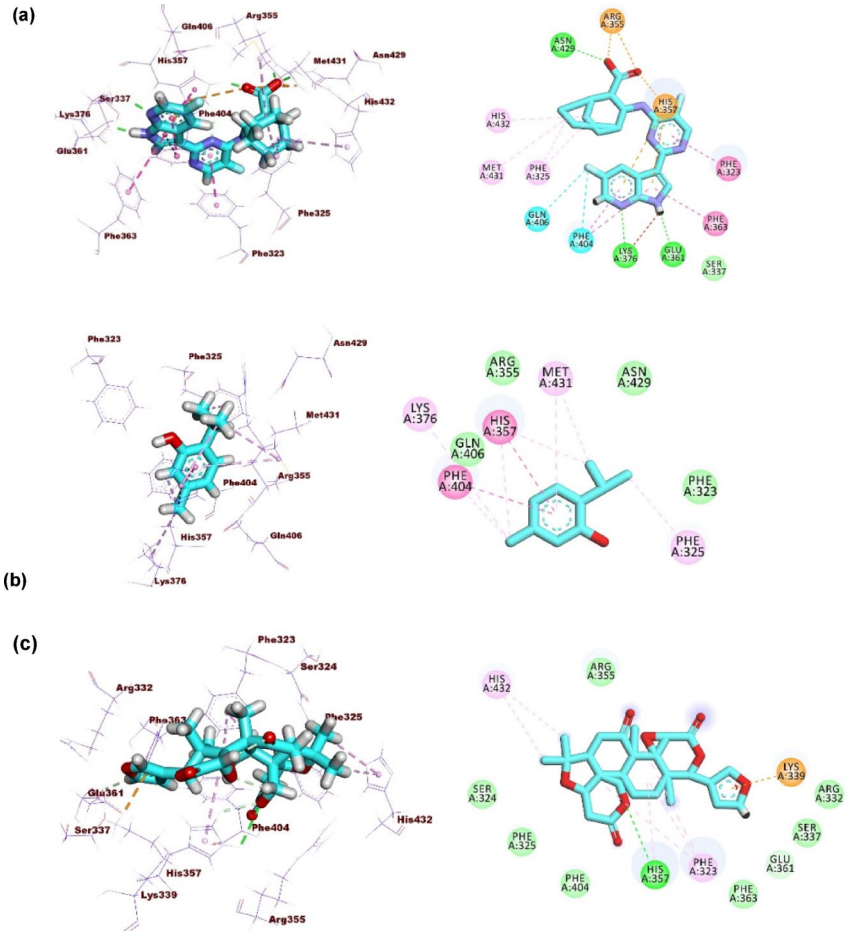

Fig. 6. (**a**) Binding mode of the co-crystallized ligand (Pimodivir) against IAV PB2 protein; (**b**) Binding mode of Thymol against IAV PB2 protein; (**c**) Binding mode of Limonin against IAV PB2 protein.

bond with His357. Additionally, it engaged in six hydrophobic interactions with His432 and Phe323. Furthermore, an electrostatic attraction was observed between Limonin and Lys339 (Fig. 6c).

Docking studies against IAV endonuclease PA protein

The co-crystallized ligand (Baloxavir acid) demonstrated a binding score of -19.43 kcal/mol against IAV PA protein. The (*R*)-7-hydroxy-3,4,12,12a-tetrahydro-1*H*-[1,4]oxazino[3,4-c]pyrido[2,1-*f*][1,2,4]triazine-6,8-dione moiety was positioned in the first pocket (zinc region) of the receptor, forming two hydrogen bonds with Leu106 and Lys134. Additionally, it established three electrostatic bonds with zinc 901 and Lys134, along with

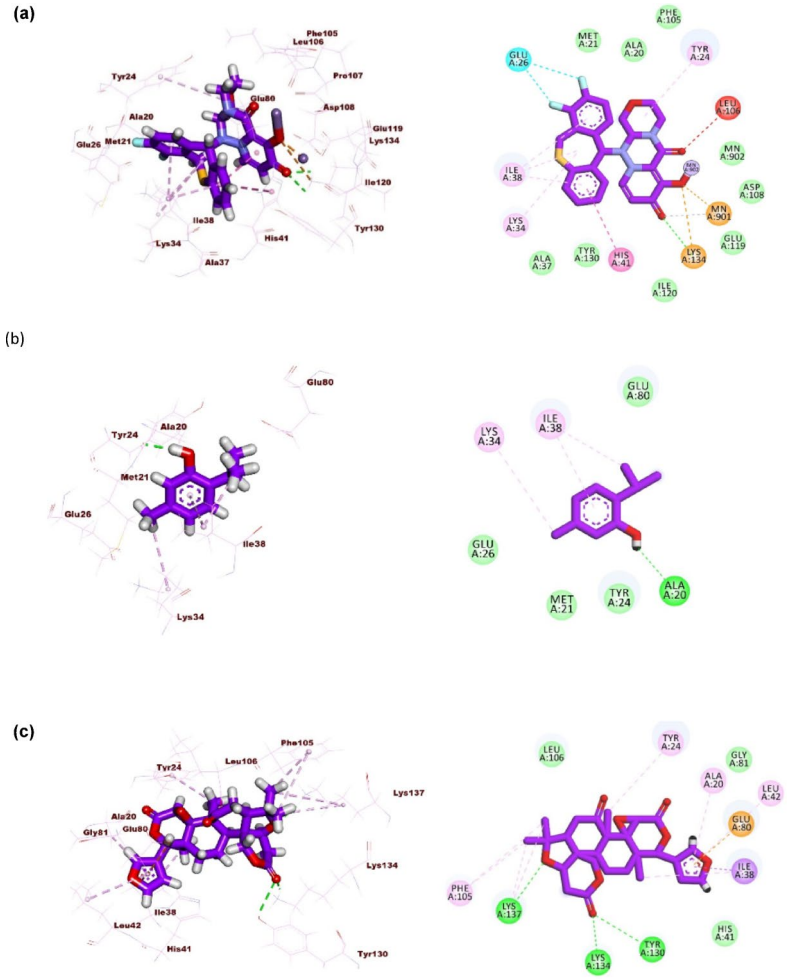

Fig. 7. (**a**) Binding mode of the co-crystallized ligand (Baloxavir acid) with IAV PA protein; (**b**) Binding mode of Thymol IAV PA protein; (**c**) Binding mode of Limonin with IAV PA protein.

a hydrophobic bond with Tyr24. The 7,8-difluoro-6,11-dihydrodibenzo[*b*,*e*]thiazine moiety occupied the outer region of the active site, creating two hydrogen bonds with Glu26 and five hydrophobic interactions with Ile38, Lys34, and His41 (Fig. 7a). Thymol displayed a weak binding mode against influenza A/pH1N1 endonuclease protein, with a binding energy of -12.52 Kcal/mol. The hydroxyl group formed a hydrogen bond with Ala20, while the isopropyl moiety engaged in one hydrophobic interaction with Ile38. The tolyl moiety formed two hydrophobic interactions with Ile38 and Lys34 (Fig. 7b). Limonin exhibited a highly efficient binding mode against influenza A/pH1N1 endonuclease protein, with a binding energy of -22.54 Kcal/mol. It formed three hydrogen bonds with Lys137, Lys134, and Tyr130. Furthermore, it engaged in nine hydrophobic interactions with Lys137, Phe105, Tyr24, Ala20, Leu42, and Ile38. Additionally, it established an electrostatic interaction with Glu80 (Fig. 7c).

Discussion

The "One-Drug-for-One-Bug" paradigm for antiviral drug development has proven effective for HIV, HCV, and influenza viruses[73]. However, broad-spectrum antivirals are desperately needed to control emerging and re-emerging viral epidemics or pandemics, such as SARS-CoV-2, seasonal influenza viruses including influenza A/H1N1, and highly pathogenic avian influenza viruses including influenza A/H5N1. Considering this, we investigated the broad-spectrum antiviral potentials of a variety of botanical EOs against three enveloped RNA respiratory viruses and found that only Thymol and Limonin have efficient antiviral activities against the three studied viruses with potent IC_{50} values and high selectivity indices (SI˃100). Thus, only Thymol and Limonin have been selected for further validation studies and interestingly, the results showed that they can reduce the viral titers by interfering primarily with the viral replication stage(s) of IAVs.

Thymol is a major component of thyme plant extract (Thymus vulgaris L., Lamiaceae), a medicinal plant known for its various therapeutic properties including antiviral activity[47,74,75]. Studies reported the antiviral potential of Thymol against A/Puerto Rico/8/1934 H1N1 and its cytotoxicity on A549 cells using

an MTT assay[75]. The MTT results revealed that the half-maximal cytotoxic concentration for Thymol on A549 cells was 49.4 µg/ml, while Quantitative real-time PCR analysis showed that the tested Thymol could effectively reduce the viral titer at concentrations of 25 µg/ml[75]. Furthermore, western blotting studies proved that Thymol affects the tested IAV strain by interfering with viral replication stages[75]. Concerning the anti-SARS-CoV-2 activity, previous reports of the antiviral activity of Thymol among other EOs revealed antiviral potential for Thymol against SARS-CoV-2 in Vero E6. The CC_{50} value in Vero E6 cells, as measured by MTT assay, was 617 µM showing highly safe use compared to other investigated EOs and the plaque reduction results showed lower viral inhibition percentages (96%) compared to the other EOs[76]. Moreover, several studies elucidated the capability of Thymol to combat viral infection, which is probably due to its phenol ring structure as previously described[49,77,78].

Different studies reported the antiviral efficacy of Limonin (or Evodin; a tetracyclic triterpene extracted from citrus fruits as a secondary metabolite with high biological activities) against a variety of DNA and RNA viruses such as HIV type-1, HSV type 1 and type 2, and the Newcastle disease virus (NDV)[52,56,58], but rare or no information was found in the literature regarding the antiviral properties of Limonin against IAVs. In silico prediction study on Limonin among other phytochemicals showed that it can bind active sites of TMPRSS2 and furin, host proteases, preventing their proteolytic cleavage activity and hence, blocking SARS-CoV-2 entry into host cells[79]. Noteworthy, Limonin is different from Limonene (or Dipentene) which is a natural monoterpene, but both are found in citrus fruit peels.

On the same hand, Camphor exerted reliable, safe use on MDCK with CC_{50} value > 10 mg/ml. The preliminary screening of the anti-influenza potential elucidated mild-to-moderate activity of Camphor against influenza A/H1N1 virus with an IC_{50} value of 234.1 µg/ml. In the light of the antiviral potential of Camphor, several reports have clearly shown the efficacy of Camphor derivatives against many strains of IAVs[51,80–83], but the antiviral potential of Camphor oil against either IAV or SARS-CoV-2 has not reported, yet. Likely, Peppermint oil has high safety on MDCK cells with CC_{50} values of 5.23 mg/ml, but with mild or no anti-influenza activity. Previous research on Peppermint oil's antiviral properties discovered that it has virucidal effects on HSV-1 and HSV-2 in RC-37 cells. According to the study, this oil may be slightly toxic to the tested cell line (RC-37), as indicated by its TC_{50} (half maximal toxic concentration) of 0.014%[38]. Nevertheless, there was little or no research on the antiviral potential of Peppermint against IAV found in the literature.

Several studies reported the antiviral potential of Eucalyptus oil against influenza viruses[84–88], but our data showed that it has no antiviral activity against the tested influenza A/H1N1 virus and it has also shown to be highly safe on MDCK with CC_{50} < 10 mg/ml. However, comparing the findings of this study to previously published research is complicated as the plant-derived oil's composition is known to vary concerning regional climatic conditions, soil conditions, and extraction techniques. Furthermore, the results obtained may differ due to the method used to evaluate antiviral activity. Commercial products rarely report oil concentration and chemical composition. Several computational studies have analyzed and described Eucalyptus oils as good antiviral agents against SARS-CoV-2 which supports our findings[89–92]. Similarly, the data obtained in this study revealed that Clove oil is highly safe on MDCK cells with CC_{50} < 10 mg/ml but it has no antiviral potential against influenza A/H1N1 virus.

The biochemical analyses and docking studies revealed significant results, demonstrating that Limonin and Thymol exhibit more effective binding within the crystal structures of influenza IAV PB2 and IAV PA proteins compared to IAV neuraminidase. These findings offer valuable insights into the antiviral mechanisms of both Thymol and Limonin. Clinical research into the potential health benefits of EOs and their pure components, such as Thymol and Limonin, is necessary. These substances may be administered as broad-spectrum antivirals to reduce the spread of enveloped respiratory viruses, ease symptoms, and possibly contribute to disease prevention. However, further investigations are needed to assess their toxicity and efficacy in animal model(s).

Conclusions

This study underscores the high demand for safe and broad-spectrum antiviral drugs, especially in the face of the concurrent threats posed by influenza epidemics/pandemics and COVID-19 pandemic. The investigation of EOs and their pure constituents revealed a potential antiviral activity of Thymol and Limonin against IAVs and SARS-CoV-2 viruses. These compounds demonstrated remarkable safety profiles in cell lines, allowing for comprehensive screening at various concentrations. Thymol and Limonin exhibited significant anti-influenza activities against both influenza A/H1N1 and A/H5N1 viruses, showcasing their broad-spectrum anti-influenza activity. Moreover, the study highlighted their promising anti-coronavirus activities against SARS-CoV-2. Biochemical analysis and *silico* molecular investigations revealed that Thymol and Limonin may target key viral proteins, obstructing active binding sites of influenza A/H1N1 PB2 and PA proteins to exert their virucidal effects. These findings provide valuable insights into the potential molecular mechanisms underlying the antiviral actions of Thymol and Limonin. Overall, the data presented in this study contribute to the development of supplementary therapeutic strategies against influenza A/H1N1, A/H5N1 and SARS-CoV-2 viruses, emphasizing the potential of Thymol and Limonin as promising antiviral candidates for further exploration and development.

Data availability

All data generated or analyzed during this study are included in this published article.

Received: 11 September 2024; Accepted: 11 June 2025
Published online: 02 July 2025

References

1. Bar-On, Y. M., Flamholz, A., Phillips, R. & Milo, R. SARS-CoV-2 (COVID-19) by the numbers. *Elife* **9**, e57309. (2020).
2. Jartti, T., Jartti, L., Ruuskanen, O. & Söderlund-Venermo, M. New respiratory viral infections. *Curr. Opin. Pulm. Med.* **18**, 271–278 (2012).
3. Boncristiani, H., Criado, M. & Arruda, E. Respiratory viruses. *Encyclopedia Microbiology* 500. (2009).
4. Vashishtha, V. M. Current status of tuberculosis and acute respiratory infections in india: much more needs to be done! *Indian Pediatr.* **47**, 88–89 (2010).
5. Peteranderl, C., Herold, S. & Schmoldt, C. Human influenza virus infections. *Semin Respir Crit. Care Med.* **37**, 487–500. https://doi.org/10.1055/s-0036-1584801 (2016).
6. Osterhaus, A. D. New respiratory viruses of humans. *Pediatr. Infect. Dis. J.* **27**, S71–S74 (2008).
7. Abdelrahman, Z., Li, M. & Wang, X. Comparative review of SARS-CoV-2, SARS-CoV, MERS-CoV, and influenza a respiratory viruses. *Frontiers Immunology* 2309. (2020).
8. Yin, Z. et al. A comparison of clinical and chest CT findings in patients with influenza A (H1N1) virus infection and coronavirus disease (COVID-19). *Am. J. Roentgenol.* **215**, 1065–1071 (2020).
9. Nishiura, H. Case fatality ratio of pandemic influenza. *Lancet. Infect. Dis.* **10**, 443–444 (2010).
10. Johnson, N. P. & Mueller, J. Updating the accounts: global mortality of the 1918–1920 Spanish influenza pandemic. *Bulletin History Medicine* 105–115. (2002).
11. Murray, C. J., Lopez, A. D., Chin, B., Feehan, D. & Hill, K. H. Estimation of potential global pandemic influenza mortality on the basis of vital registry data from the 1918–20 pandemic: a quantitative analysis. *Lancet* **368**, 2211–2218 (2006).
12. Kumar, A. et al. Wuhan to world: the COVID-19 pandemic. *Front. Cell. Infect. Microbiol.* **11** https://doi.org/10.3389/fcimb.2021.596201 (2021).
13. Enserink, M. & Cohen, J. The novel H1N1 influenza. (2009).
14. Lazarus, J. V. et al. A survey of COVID-19 vaccine acceptance across 23 countries in 2022. *Nat. Med.* https://doi.org/10.1038/s41591-022-02185-4 (2023).
15. Excler, J. L., Saville, M., Berkley, S. & Kim, J. H. Vaccine development for emerging infectious diseases. *Nat. Med.* **27**, 591–600. https://doi.org/10.1038/s41591-021-01301-0 (2021).
16. Ren, H. & Zhou, P. Epitope-focused vaccine design against influenza A and B viruses. *Curr. Opin. Immunol.* **42**, 83–90 (2016).
17. Baby, K. et al. Targeting SARS-CoV-2 main protease: a computational drug repurposing study. *Arch. Med. Res.* **52**, 38–47 (2021).
18. Shahabadi, N., Zendehcheshm, S., Mahdavi, M. & Khademi, F. Repurposing FDA-approved drugs cetilistat, abiraterone, diiodohydroxyquinoline, bexarotene, and Remdesivir as potential inhibitors against RNA dependent RNA polymerase of SARS-CoV-2: A comparative in Silico perspective. *Inf. Med. Unlocked*. **36**, 101147 (2023).
19. Shoaib, S. et al. An attention towards the prophylactic and therapeutic options of phytochemicals for SARS-CoV-2: A molecular insight. *Molecules* **28**, 795 (2023).
20. Pizzorno, A. et al. Repurposing of drugs as novel influenza inhibitors from clinical gene expression infection signatures. *Front. Immunol.* **10**, 60 (2019).
21. Newman, D. J. & Cragg, G. M. Natural products as sources of new drugs from 1981 to 2014. *J. Nat. Prod.* **79**, 629–661 (2016).
22. Shokry, S.; Hegazy, A.; Abbas, A.M.; Mostafa, I.; Eissa, I.H.; Metwaly, A.M.; Yahya,G.; El-Shazly, A.M.; Aboshanab, K.M.; Mostafa, A. Phytoestrogen β-Sitosterol Exhibits Potent In Vitro Antiviral Activity against Influenza A Viruses. *Vaccines* 2023, *11*, 228.
23. Hegazy, A. et al. Robust antiviral activity of Santonica flower extract (Artemisia cina) against avian and human influenza A viruses: in vitro and chemoinformatic studies. *ACS Omega*. **7**, 41212–41223. https://doi.org/10.1021/acsomega.2c04867 (2022).
24. Hegazy, A. et al. Antiviral activities of plant-derived Indole and β-carboline alkaloids against human and avian influenza viruses. *Sci. Rep.* **13**, 1612. https://doi.org/10.1038/s41598-023-27954-0 (2023).
25. Chouhan, S., Sharma, K. & Guleria, S. Antimicrobial activity of some essential Oils-Present status and future perspectives. *Med. (Basel)*. **4** https://doi.org/10.3390/medicines4030058 (2017).
26. Bunse, M. et al. Essential oils as multicomponent mixtures and their potential for human health and Well-Being. *Front. Pharmacol.* **13** https://doi.org/10.3389/fphar.2022.956541 (2022).
27. Pathania, D. et al. Essential oil derived biosynthesis of metallic nano-particles: implementations above essence. *Sustainable Mater. Technol.* **30**, e00352 (2021).
28. Li, Y., Fabiano-Tixier, A. S. & Chemat, F. *Essential oils as reagents in green chemistry*; Springer: ; Volume 1. (2014).
29. Sharifi-Rad, J. et al. Biological activities of essential oils: from plant chemoecology to traditional healing systems. *Molecules* **22**, 70 (2017).
30. El Omari, K. et al. In-vitro evaluation of the antibacterial activity of the essential oils of Micromeria barbata, Eucalyptus globulus and Juniperus excelsa against strains of Mycobacterium tuberculosis (including MDR), Mycobacterium kansasii and Mycobacterium gordonae. *J. Infect. Public Health*. **12**, 615–618 (2019).
31. Elshafie, H. S. & Camele, I. An overview of the biological effects of some mediterranean essential oils on human health. *BioMed research international 2017*. (2017).
32. Seol, G. H. & Kim, K. Y. Eucalyptol and its role in chronic diseases. *Drug Discovery Mother. Nature* 389–398. (2016).
33. Rozza, A. L. & Pellizzon, C. H. Essential oils from medicinal and aromatic plants: a review of the gastroprotective and ulcer-healing activities. *Fundam. Clin. Pharmacol.* **27**, 51–63 (2013).
34. Buckle, J. *Clinical aromatherapy-e-book: essential oils in practice*; Elsevier Health Sciences: (2014).
35. Kandeil, A. et al. Coding-Complete genome sequences of two SARS-CoV-2 isolates from Egypt. *Microbiol. Resource Announcements*. **9** (2020).
36. Reed, L. J. & Muench, H. A simple method of estimating Fifty per cent endpoints. *Am. J. Epidemiol.* **27**, 493–497 (1938).
37. Hamdan, D. et al. Chemical composition and biological activity of Citrus jambhiri lush. *Food Chem.* **127**, 394–403. https://doi.org/10.1016/j.foodchem.2010.12.129 (2011).
38. Schuhmacher, A., Reichling, J. & Schnitzler, P. Virucidal effect of peppermint oil on the enveloped viruses herpes simplex virus type 1 and type 2 in vitro. *Phytomedicine* **10**, 504–510 (2003).
39. Rajan, S. Development of novel microemulsion-based topical formulations of acyclovir for the treatment of cutaneous herpetic infections. *AAPS PharmSciTech*. **10**, 559–565 (2009).
40. Rosato, A. et al. Elucidation of the synergistic action of Mentha Piperita essential oil with common antimicrobials. *PloS One*. **13**, e0200902 (2018).
41. Cermelli, C., Fabio, A., Fabio, G. & Quaglio, P. Effect of eucalyptus essential oil on respiratory bacteria and viruses. *Curr. Microbiol.* **56**, 89–92 (2008).
42. Brochot, A., Guilbot, A., Haddioui, L. & Roques, C. Antibacterial, antifungal, and antiviral effects of three essential oil blends. *Microbiologyopen* **6**, e00459 (2017).
43. Tragoolpua, Y. & Jatisatienr, A. Anti-herpes simplex virus activities of Eugenia caryophyllus (Spreng.) Bullock & SG Harrison and essential oil, Eugenol. *Phytotherapy Research: Int. J. Devoted Pharmacol. Toxicol. Evaluation Nat. Prod. Derivatives*. **21**, 1153–1158 (2007).

44. El-Saber Batiha, G. et al. Syzygium aromaticum L.(Myrtaceae): traditional uses, bioactive chemical constituents, Pharmacological and toxicological activities. *Biomolecules* **10**, 202 (2020).
45. Han, X. & Parker, T. L. Anti-inflammatory activity of clove (Eugenia caryophyllata) essential oil in human dermal fibroblasts. *Pharm. Biol.* **55**, 1619–1622 (2017).
46. Li, Y. et al. -w. Thymol inhibits bladder cancer cell proliferation via inducing cell cycle arrest and apoptosis. *Biochem. Biophys. Res. Commun.* **491**, 530–536 (2017).
47. Lai, W. L. et al. Inhibition of herpes simplex virus type 1 by thymol-related monoterpenoids. *Planta Med.* **78**, 1636–1638 (2012).
48. Kulkarni, S. A. et al. Computational evaluation of major components from plant essential oils as potent inhibitors of SARS-CoV-2 Spike protein. *J. Mol. Struct.* **1221**, 128823 (2020).
49. Vimalanathan, S. & Hudson, J. Anti-influenza virus activity of essential oils and vapors. *Am. J. Essent. Oils Nat. Prod.* **2**, 47–53 (2014).
50. Karaca, N., Şener, G., Demirci, B. & Demirci, F. Synergistic antibacterial combination of Lavandula latifolia medik. Essential oil with Camphor. *Z. Für Naturforschung C.* **76**, 169–173 (2021).
51. Kovaleva, K. S. et al. Synthesis of D-(+)-camphor-based N-acylhydrazones and their antiviral activity. *Medchemcomm* **9**, 2072–2082 (2018).
52. Abd, A. J., Al-Shammarie Ahmed, M. & Abd, A. H. H. Antiviral activity of Limonin against Newcastle disease virus in vitro. *Res. J. Biotechnol.* **14**, 320–328 (2019).
53. Gualdani, R., Cavalluzzi, M. M., Lentini, G. & Habtemariam, S. The chemistry and Pharmacology of Citrus limonoids. *Molecules* **21**, 1530 (2016).
54. Chidambara Murthy, K. N., Jayaprakasha, G. K. & Patil, B. S. Citrus limonoids and Curcumin additively inhibit human colon cancer cells. *Food Funct.* **4**, 803–810. https://doi.org/10.1039/C3FO30325J (2013).
55. Fan, S. et al. Limonin: A review of its pharmacology, toxicity, and pharmacokinetics. *Molecules* **24**, 3679 (2019).
56. Battinelli, L. et al. Effect of Limonin and nomilin on HIV-1 replication on infected human mononuclear cells. *Planta Med.* **69**, 910–913 (2003).
57. Berretta, A. A., Silveira, M. A. D., Capcha, J. M. C. & De Jong, D. Propolis and its potential against SARS-CoV-2 infection mechanisms and COVID-19 disease: running title: Propolis against SARS-CoV-2 infection and COVID-19. *Biomed. Pharmacother.* **131**, 110622 (2020).
58. Chansriniyom, C., Ruangrungsi, N., Lipipun, V., Kumamoto, T. & Ishikawa, T. Isolation of acridone alkaloids and N-[(4-monoterpenyloxy) phenylethyl]-substituted sulfur-containing propanamide derivatives from Glycosmis Parva and their anti-herpes simplex virus activity. *Chem. Pharm. Bull.* **57**, 1246–1250 (2009).
59. Mahmoud, A. et al. Telaprevir is a potential drug for repurposing against SARS-CoV-2: computational and in vitro studies. *Heliyon* **7**, e07962 (2021).
60. Mostafa, A. et al. FDA-approved drugs with potent in vitro antiviral activity against severe acute respiratory syndrome coronavirus 2. *Pharmaceuticals* **13**, 443 (2020).
61. Mostafa, A. et al. FDA-Approved drugs with potent in vitro antiviral activity against severe acute respiratory syndrome coronavirus 2. *Pharmaceuticals (Basel Switzerland).* **13** https://doi.org/10.3390/ph13120443 (2020).
62. Gaush, C. R. & Smith, T. F. Replication and plaque assay of influenza virus in an established line of canine kidney cells. *Appl. Microbiol.* **16**, 588–594 (1968).
63. Bayoumi, M. et al. Identification of amino acid residues responsible for differential replication and pathogenicity of avian influenza virus H5N1 isolated from human and cattle in texas, US. *bioRxiv* 2025, 2025.2003.2001.640810, https://doi.org/10.1101/2025.03.01.640810
64. Alesawy, M. S. et al. In Silico studies of some isoflavonoids as potential candidates against COVID-19 targeting human ACE2 (hACE2) and viral main protease (Mpro). *Molecules* **26**, 2806 (2021).
65. Hagras, M. et al. Discovery of new Quinolines as potent Colchicine binding site inhibitors: design, synthesis, Docking studies, and anti-proliferative evaluation. *J. Enzyme Inhib. Med. Chem.* **36**, 640–658 (2021).
66. Alanazi, M. M. et al. New Bis ([1, 2, 4] triazolo)[4, 3-a: 3′, 4′-c] Quinoxaline derivatives as VEGFR-2 inhibitors and apoptosis inducers: design, synthesis, in Silico studies, and anticancer evaluation. *Bioorg. Chem.* **112**, 104949 (2021).
67. Li, Y., Han, L., Liu, Z. & Wang, R. Comparative assessment of scoring functions on an updated benchmark: 2. Evaluation methods and general results. *J. Chem. Inf. Model.* **54**, 1717–1736 (2014).
68. Pawar, S. S. & Rohane, S. H. Review on discovery studio: an important tool for molecular Docking. *Asian J. Res. Chem.* **14**, 86–88 (2021).
69. Yousef, R. G. et al. New quinoxaline-2 (1 H)-ones as potential VEGFR-2 inhibitors: design, synthesis, molecular docking, ADMET profile and anti-proliferative evaluations. *New J. Chem.* **45**, 16949–16964 (2021).
70. Alesawy, M. S., Elkaeed, E. B., Alsfouk, A. A., Metwaly, A. M. & Eissa, I. H. In Silico screening of semi-synthesized compounds as potential inhibitors for SARS-CoV-2 papain-like protease: pharmacophoric features, molecular docking, ADMET, toxicity and DFT studies. *Molecules* **26**, 6593 (2021).
71. Shokry, S. et al. Phytoestrogen β-Sitosterol exhibits potent in vitro antiviral activity against influenza A viruses. *Vaccines* **11** https://doi.org/10.3390/vaccines11020228 (2023).
72. Barakat, A. et al. Synthesis and in vitro evaluation of Spirooxindole-Based phenylsulfonyl moiety as a candidate Anti-SAR-CoV-2 and MERS-CoV-2 with the implementation of combination studies. *Int. J. Mol. Sci.* **23** https://doi.org/10.3390/ijms231911861 (2022).
73. Vigant, F., Santos, N. C. & Lee, B. Broad-spectrum antivirals against viral fusion. *Nat. Rev. Microbiol.* **13**, 426–437 (2015).
74. Lenz, E. et al. Authorised medicinal product Aspecton® oral drops containing thyme extract KMTv24497 shows antiviral activity against viruses which cause respiratory infections. *J. Herb. Med.* **13**, 26–33. https://doi.org/10.1016/j.hermed.2018.02.003 (2018).
75. Nandi, T. & Khanna, M. Anti-Viral activity of thymol against influenza A virus. *EC Microbiol.* **18**, 98–103 (2022).
76. Seadawy, M. G. et al. A.R.N. In vitro: natural compounds (Thymol, Carvacrol, Hesperidine, and Thymoquinone) against Sars-Cov2 strain isolated from Egyptian patients. *bioRxiv* 2020.2011. 2007.367649. (2020).
77. Saad, N. Y., Muller, C. D. & Lobstein, A. Major bioactivities and mechanism of action of essential oils and their components. *Flavour Fragr. J.* **28**, 269–279 (2013).
78. da Silva, J. K. R., Figueiredo, P. L. B., Byler, K. G. & Setzer, W. N. Essential oils as antiviral agents, potential of essential oils to treat SARS-CoV-2 infection: an In-Silico investigation. *Int. J. Mol. Sci.* **21**, 3426 (2020).
79. Vardhan, S. & Sahoo, S. K. Virtual screening by targeting proteolytic sites of Furin and TMPRSS2 to propose potential compounds obstructing the entry of SARS-CoV-2 virus into human host cells. *J. Traditional Complement. Med.* **12**, 6–15 (2022).
80. Sokolova, A. S. et al. Aliphatic and alicyclic Camphor Imines as effective inhibitors of influenza virus H1N1. *Eur. J. Med. Chem.* **127**, 661–670 (2017).
81. Sokolova, A. S. et al. New quaternary ammonium Camphor derivatives and their antiviral activity, genotoxic effects and cytotoxicity. *Bioorg. Med. Chem.* **21**, 6690–6698 (2013).
82. Zarubaev, V. et al. Broad range of inhibiting action of novel camphor-based compound with anti-hemagglutinin activity against influenza viruses in vitro and in vivo. *Antiviral Res.* **120**, 126–133 (2015).
83. Kovaleva, K. S. et al. Synthesis and antiviral activity of N-heterocyclic hydrazine derivatives of Camphor and Fenchone. *Chem. Heterocycl. Compd.* **57**, 455–461 (2021).

84. Pyankov, O. V., Usachev, E. V., Pyankova, O. & Agranovski, I. E. Inactivation of airborne influenza virus by tea tree and Eucalyptus oils. *Aerosol Sci. Technol.* **46**, 1295–1302. https://doi.org/10.1080/02786826.2012.708948 (2012).
85. Madia, V. N. et al. Di santo, R. Ultrastructural damages to H1N1 influenza virus caused by vapor essential oils. *Molecules* **27**, 3718 (2022).
86. Sadatrasul, M. S. et al. Oil-in-water emulsion formulated with eucalyptus leaves extract inhibit influenza virus binding and replication in vitro. *AIMS Microbiol.* **3**, 899 (2017).
87. Najar, B. et al. Screening of the essential oil effects on human H1N1 influenza virus infection: an in vitro study in MDCK cells. *Nat. Prod. Res.* **36**, 3149–3152 (2022).
88. Mieres-Castro, D., Ahmar, S., Shabbir, R. & Mora-Poblete, F. Antiviral activities of eucalyptus essential oils: their effectiveness as therapeutic targets against human viruses. *Pharmaceuticals* **14**, 1210 (2021).
89. Wilkin, P. J., Al-Yozbaki, M., George, A., Gupta, G. K. & Wilson, C. M. The undiscovered potential of essential oils for treating SARS-CoV-2 (COVID-19). *Curr. Pharm. Design.* **26**, 5261–5277 (2020).
90. González-Maldonado, P. et al. Cantero-González, G. Screening of natural products inhibitors of SARS-CoV-2 entry. *Molecules* **27**, 1743 (2022).
91. Sharma, A. D. & Kaur, I. Eucalyptus essential oil bioactive molecules from against SARS-CoV-2 Spike protein: insights from computational studies. (2021).
92. dev Sharma, A. Homology modeling and molecular Docking of natural metabolites from eucalyptus essential oil against SARS-CoV-2 Spike protein. *Arab. J. Med. Aromatic Plants.* **7**, 282–303 (2021).

Acknowledgements

The authors would like to acknowledge the funding by the Deanship of Scientific Research at Jouf University under Grant Number (DSR2022-RG-0152).

Author contributions

Conceptualization, G.M-H, A.H., L.M-S., and A.M.; methodology, G.M-H, A.H., I.M., I.H.E., A.M.M., H.A.E., A.Y.E., S.H.A., A.O.E.A., F.O.A., M.F.A.A., T.A.M., M.A., A.M.S., M.B., A.M.E. and A.M.; software, I.H.E. and A.M.M.; validation, G.M-H, A.H., A.M.E., A.O.E.A., I.H.E., A.M.M., F.O.A. and A.M.; formal analysis, G.M-H, A.H., A.M.S., A.M.E., L.M-S. and A.M.; investigation, G.M-H, A.H., A.M.E. and A.M.; resources, G.M-H, L.M-S. and A.M.; data curation, G.M-H, A.H. and A.M.; writing—original draft preparation, G.M-H, A.H. and A.M.; writing—review and editing, G.M-H, A.H., L.M-S. and A.M.; visualization, G.M-H, A.H. and A.M.; supervision, G.M-H and A.M.; project administration, G.M-H and A.M.; funding acquisition, G.M-H., L.M-S. and A.M. All authors have read and agreed to the published version of the manuscript.

Funding

This work was funded by the Deanship of Scientific Research at Jouf University under Grant Number (DSR2022-RG-0152, to G.M-H.). This work was also supported by a grant from the American Lung Association (ALA, to L.M-S) and Texas Biomed Forum (Award # 1520001, to A.M.). The funders had no role in study design, data collection and analysis, decision to publish, or preparation of the manuscript.

Declarations

Competing interests

The authors declare no competing interests.

Additional information

Correspondence and requests for materials should be addressed to G.M.-H., L.M.-S. or A.M.